Osteoarthritis and Cartilage (2007) **15,** 1388–1396

doi:10.1016/j.joca.2007.05.003

Osteoarthritis and Cartilage

International Cartilage Repair Society

OARSI OSTEOARTHRITIS RESEARCH SOCIETY INTERNATIONAL

Laser scanning confocal arthroscopy of a fresh cadaveric knee joint

C. W. Jones B.Eng. (Hons.), B.Com.†, D. Smolinski B.Eng. (Hons.)†, C. Willers B.Sc. (Hons.), M.(Med.)Sc.‡, P. J. Yates M.B.B.S. (Hons.), B.Sc. (Hons.), M.R.C.S., F.R.C.S.‡, A. Keogh M.B.B.S. (Hons.), B.Sc. (Hons.)‡, D. Fick M.B.B.S. (Hons.), B.Sc. (Hons.)‡, T. B. Kirk Ph.D., B.Eng. (Hons.)† and M. H. Zheng Ph.D., D.M., F.R.C.Path.‡*

† *School of Mechanical Engineering, University of Western Australia, 35 Stirling Highway, Crawley, WA 6009, Australia*

‡ *School of Pathology and Surgery, Department of Orthopaedics, University of Western Australia, 2nd Floor M-block QEII Medical Centre, Nedlands, Perth, WA 6009, Australia*

Summary

Objective: Osteoarthritis (OA) inflicts an enormous burden upon sufferers and healthcare systems worldwide. Continuing efforts to elucidate the aetiology of OA have indicated the need for non-destructive methods of *in vivo* microstructural assessment of articular cartilage (AC). In this study, we describe the first use of a recently developed laser scanning confocal arthroscope (LSCA) to image the cartilage of a fresh frozen cadaveric knee from a patient with OA.

Design: Using an adaptation of the International Cartilage Repair Society (ICRS) joint mapping protocol, the joint was divided into three discrete regions (femoral condyle, patella and tibial plateau) for grading according to the ICRS (Outerbridge) system. The LSCA was used to generate images from each area within the three regions. Following imaging, the joint was sectioned and histology was performed on the corresponding sites with histological grading (modified-Mankin).

Results: Quantitative results of ICRS, LSCA and histological OA assessment were compared using intraclass correlation (ICC) and Pearson correlation analysis. The LSCA enabled visualisation of chondrocyte morphology and cell density, with classical OA changes such as chondrocyte clustering, surface fibrillation and fissure formation evident. Obvious qualitative similarities between LSCA images and histology were observed, with fair to moderate agreement ($P < 0.05$) demonstrated between modalities.

Conclusions: In this study, we have shown the viability of the LSCA for non-destructive imaging of the microstructure of OA knee cartilage. LSCA technology is potentially a valuable research and clinical tool for the non-destructive assessment of AC microstructure in early to late OA.

Key words: Osteoarthritis, Articular cartilage, Confocal microscopy.

Introduction

Articular cartilage (AC) is a tissue of remarkable biomechanical properties able to both absorb and dissipate joint loads, while providing an almost frictionless bearing surface. AC has a zonal organisation that is essential to its physiological function, with depth-dependant cellular distribution, biochemical composition and mechanical properties[1,2]. Cartilage degeneration during the progression of osteoarthritis (OA) causes significant burden to both individual sufferers and healthcare systems worldwide[3,4]. The gradual erosion of AC leads to pain, stiffness and disability[5].

Although sparsely represented with less than 2% cell volume density, the mechanotransductive role of the chondrocyte is central to AC health. Chondrocytes are responsible for the synthesis and maintenance of the collagen and proteoglycan (PG) rich extracellular matrix (ECM)[1,2,6]. Evidence suggests that following an initial insult, the chondrocyte proliferation and clustering seen in early OA may be a reparative attempt to bolster matrix synthesis[7]. During the course of the disorder, cell densities are seen to diminish, with consequential ECM deterioration manifesting as a loss of the superficial layer and the development of collagen fibrillation. Later, complete erosion of the chondral surface can be observed, with involvement sometimes extending into subchondral bone[8–11].

While much is known regarding the course of established OA, details regarding the exact aetiological initiation remain elusive[5]. Current opinion suggests a multifactorial combination of genetic and environmental influences leading to chondrocyte death, PG loss and collagen matrix destruction[12]. Elucidating the exact pathophysiology of the initial stages of OA requires detailed information of tissue microstructural

*Address correspondence and reprint requests to: Prof Ming-Hao Zheng, Ph.D., D.M., F.R.C.Path., Orthopaedic Research Laboratories, Department of Orthopaedic Surgery, School of Surgery and Pathology, University of Western Australia, Nedlands, WA 6009, Australia. Tel: 61-407982570; E-mail: cjon0040@med.usyd.edu.au, daniel.smolinski@dsto.defence.gov.au, craig.willers@uwa.edu.au, pyates@meddent.uwa.edu.au, guskeogh@bigpond.net.au, dfick@mac.com, kirk@mech.uwa.edu.au, minghao.zheng@uwa.edu.au
Received 19 October 2006; revision accepted 1 May 2007.

changes, heretofore provided only by conventional histological techniques. However, as cautioned by Poole[13], the limitation of taking histological biopsy samples is the inherent tissue destruction induced, and the subsequent cartilage pathology this may induce. This well-recognised limitation has previously seen the development of various non-destructive AC imaging and OA assessment techniques, including arthroscopic evaluation, roentgenography, computed tomography (CT), optical coherence tomography (OCT) and magnetic resonance imaging (MRI)[14,15]. Unfortunately, these techniques provide little detailed information on a cellular level with limited sensitivity to early OA changes. Hence, simple video arthroscopy currently remains the gold standard for non-destructive OA assessment[16,17].

We have recently developed a novel laser scanning confocal arthroscope (LSCA) for the non-destructive imaging of orthopaedic tissues; principally AC[18,19]. This technology has most recently been applied to the follow-up evaluation of matrix-induced autologous chondrocyte implantation (MACI)[20]. The LSCA is capable of acquiring high resolution three-dimensional (3D) images by utilising a miniaturised laser-scanning mechanism, that enables arthroscopic use of this innovative imaging tool[21,22]. Future disorder modifying interventions will require long-term follow-up and monitoring, preferably by non-destructive means, and in this capacity the LSCA provides a validated method for both visualising and quantifying OA progression.

In this study, we report on the unique application of the LSCA for the arthroscopic imaging of the chondral surfaces of an intact, fresh frozen osteoarthritic cadaver knee. We aimed to qualitatively and quantitatively compare LSCA scoring outcomes of a knee to arthroscopic [International Cartilage Repair Society (ICRS)] and histological assessment (modified-Mankin) of cartilage from corresponding sites.

Methods

An intact right knee was obtained from a fresh frozen cadaver purchased through the Clinical Technology and Education Centre (CTEC), University of Western Australia under strict National Health and Medical Research Council (NHMRC) guidelines governing the handing of cadaveric material. The knee was retrieved from an 80 kg 70-year-old male and had been fresh frozen without formalin fixation. The limb was severed mid femur and mid tibia, allowed to thaw at room temperature, then mounted *via* the distal femur in a surgical vice. Contrast agent (acridine orange) was introduced into the synovial capsule *via* intra-articular injection and the joint was manually manipulated for 20 min in flexion and extension. Arthroscopic video examination of the joint was performed *via* standard anterolateral and anteromedial portals with thorough lavage (0.9% phosphate buffered saline) until contrast agent staining was no longer evident in the wash-out. LSCA imaging of the joint was performed under arthroscopic video guidance, before the joint was opened *via* a medial parapatellar approach to allow for LSCA imaging in anatomically difficult regions and sectioning for histology. Using a previously described protocol[23], the knee joint surfaces were divided into three large areas (femoral condyles, tibial plateau and the patella), before being further segmented into 47 distinct areas ($N = 47$) (Fig. 1). This simply devised mapping system enabled precise lesion location and direct comparison between assessment modalities. LSCA images were compared to the ICRS (Outerbridge) arthroscopic classifications for degenerative changes in cartilage of the knee, as well as conventional histology (modified-Mankin) of the tissue retrieved from the same sites.

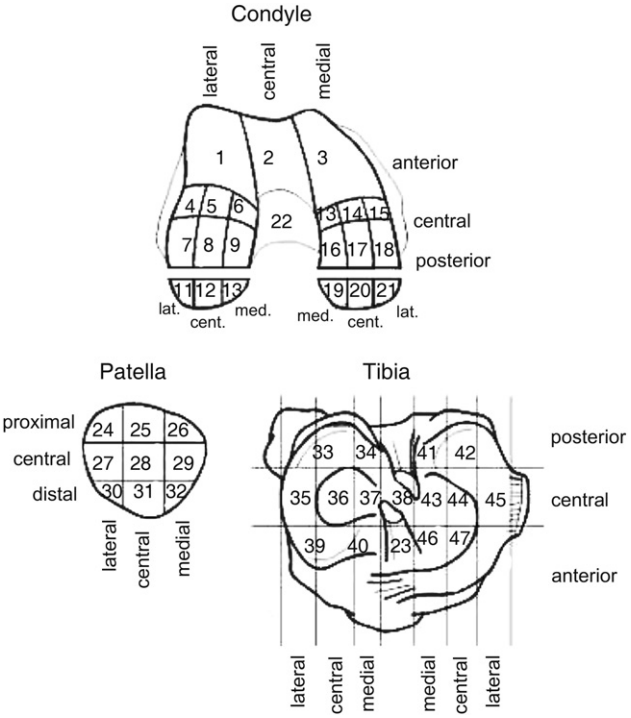

Fig. 1. Joint mapping protocol. The knee joint is divided into three areas (femoral condyles, tibial plateau and patella), and 47 individual sectors. Image adapted from the ICRS Cartilage Evaluation Package [www.cartilage.org].

ICRS CLASSIFICATION

The Outerbridge arthroscopic cartilage lesion classification system divides lesions into Grades I–IV and is widely employed for the assessment of cartilage injury[24]. Recently the ICRS has ratified Outerbridge's arthroscopic grading parameters for the evaluation of cartilage lesions[23]. Recognised limitations of this system include the provision of little information regarding lesion depth or tissue microstructural organisation. In this study, ICRS classification of cartilage lesions was made under video arthroscopy by an experienced orthopaedic surgeon prior to the introduction of fluorescent contrast agent.

LSCA

Confocal microscopy has been widely utilised across many aspects of orthopaedic research, particularly for the investigation of AC[19]. The LSCA uses an optical fibre scanner that performs both as the laser delivery and returning fluorescence vehicle and as the confocal pinhole and filtration mechanism[22]. The LSCA is 4.4 mm in diameter, employing a Class 3R solid-state laser (excitation wavelength of 488 nm, 1.0 mW at the tip, 515 nm long pass filter) producing 40× magnification across a field of view of 500×500 μm (512×512 pixels) with an *XY* spatial resolution of 2 μm to a depth of 200 μm (as measured previously in ovine and porcine cartilage)[18].

Fluorescent contrast was introduced *via* intra-articular injection of acridine orange (0.5 g/L in 0.9% PBS, 60 mL, 37°C, pH 7.4, 20 min) prior to imaging. Optimal staining concentration, volume and times were established during the course of previous study[18]. Acridine orange (*Molecular Probes* Inc., Eugene, OR, USA) provides a high contrast

"positive" image by specific DNA binding and has been previously used to assess chondrocyte cellular density and morphology[25,26]. Following acquisition, representative images from each of the 47 sections were blinded and scored according to an LSCA cartilage assessment scoring protocol developed specifically for this study (Table I). The variables of interest included the degree of cellularity (cell density), the spatial uniformity of cells, cellular distribution, cell morphology and the visibility of collagen fibres. These variables were chosen as measures of AC repair integrity in comparison to the characteristics of native (healthy) AC. After scoring, images were unblinded and scores collated and graded (I–IV) for further comparison to the other investigative modalities (ICRS and modified-Mankin grading).

HISTOLOGY AND IMMUNOHISTOCHEMISTRY

Following LSCA imaging, the knee was sectioned according to the lesion mapping system, with sections labelled and fixed in 4% paraformaldehyde. Following fixation, specimens were decalcified (10% formic acid), dehydrated (alcohol, xylene washes) and paraffin-embedded. Specimens were sectioned to 5 μm and stained by haematoxylin and eosin (H&E), alcian blue (AB), and type II collagen immunohistochemistry. Type II collagen immunohistochemistry sections were deparaffinised with xylene and rehydrated with decreasing ethanol solutions and rinsed in distilled water. After buffer preheating, sections were microwave heated in pH 6 citrate buffer at low power for antigen retrieval. Sections were then rinsed in 3% H_2O_2 in methanol to block endogenous peroxidase activity. Non-specific staining was blocked by rinsing sections in 10% fetal bovine serum (FBS) in 0.1% triton X100 in tris-buffered saline (TBS), before incubation with primary monoclonal anti-human (1:100) collagen type II mouse IgG diluted in 0.1% triton X100/1% bovine serum albumin (BSA) in TBS. After washing in TBS, sections were incubated with EnVision+ goat anti-mouse Ig peroxidase system at room temperature. Sections were washed in TBS and incubated in liquid diaminobenzidine (DAB) (2% chromophore). Sections were washed in distilled water, counterstained shortly with haematoxylin, washed, stained shortly with Scott's tap water, washed in distilled water, then dehydrated in alcohol, cleared in xylene and mounted in DePex media. Sections were viewed under light microscope and graded using the modified-Mankin scoring system as previously described[27].

STATISTICAL ANALYSIS

Interpretation between assessment modalities was made according to the OA assessment schema as detailed in

Table I
LSCA and histological OA scoring system

LSCA scoring system		Modified-Mankin scoring system	
Criteria	Score	Criteria	Score
1. Cellularity		1. Structure	
• High density	4	• Normal	12
• Moderate density	3	• Surface irregularities	10
• Low density	2	• Pannus and surface irregularity	8
• Acellular	1	• Clefts to transitional zone	6
2. Spatial uniformity of cells		• Clefts to radial zone	4
• Uniform	4	• Clefts to calcified zone	2
• Almost uniform	3	• Complete disorganisation	0
• Heterologous uniformity	2		
• Non-uniform	1	2. Cells in superficial/transitional zone	
• Acellular	0	• Normal	6
3. Cell clustering		• Diffuse hypercellularity	4
• No clustering	3	• Clonal clustering	2
• Sporadic clustering	2	• Hypocellularity	0
• Predominant clustering	1		
• Acellular	0		
4. Cell morphology			
• Predominantly spherical	3		
• Mixed morphology	2		
• Predominantly spindle-shaped	1		
• Acellular	0		
5. Visibility of collagen fibres			
• No fibres	3		
• Some fibres	2		
• Highly fibrous	1		

OA assessment

OA grade	State of cartilage	Modified-Mankin	LSCA
• Normal	Healthy	>16	>16
• Grade I	Nearly normal	11–14	12–15
• Grade II	Abnormal	7–10	9–11
• Grade III	Severely abnormal	3–6	6–8
• Grade IV	Degenerate	<3	<6

Table I. For each of the 47 sections, LSCA and modified-Mankin scores were converted to overall OA Grades I–IV, thereby enabling qualitative comparison and statistical analysis. SPSS (SPSS 11.0, *SPSS Inc.*, USA) was used to perform intraclass correlation (ICC) analysis between ICRS, LSCA and histological grading. An alpha, fully-crossed two-way analysis of variance (ANOVA) mixed model ICC design was employed, generating both a one-way random effect model (assuming people effect random) and an average measure of ICC. The ICC is a reliability procedure used to estimate inter-modality reliability based on mean squares obtained by applying sequential ANOVA while accounting for any agreement based on chance (''perfect agreement'' 1.0, ''almost perfect agreement'' 1.0–0.81, ''substantial agreement'' 0.8–0.61, ''fair agreement'' 0.6–0.41, ''moderate agreement'' 0.4–0.21, ''poor agreement'' 0.2–0.01, ''chance agreement'' 0.0, ''perfect disagreement'' −1.0)[28]. Pearson correlation coefficients were calculated to examine the direct correlation between both raw score and the overall OA assessment grades (Table II).

Results

ARTHROSCOPIC ASSESSMENT

In keeping with the known clinical diagnosis, ICRS assessment of the knee found widespread OA changes throughout the entire joint. Particular focal changes were noted on the central load-bearing regions of the femoral condyles (Grades II–III), across the distal and medial aspect of the patella (Grades III–IV), and on the centro-medial and centro-lateral load-bearing aspects of the tibial plateau (Grades II–III) (Fig. 2).

LSCA ASSESSMENT

Classical degenerative changes such as clustered chondrocytes, fissures, and surface fibrillations were readily imaged across all areas (Figs. 3 and 4). Cell clustering in lower grade OA was more easily discernable with LSCA than with conventional histology, and the organisation of cell clustering in fibrillated cartilage was better illustrated by superior view LSCA imaging than by sagittal view histology. Image scoring suggested widespread OA changes across all joint surfaces, with particular degeneration (LSCA Grade > II) noted about the weight-bearing surface of the condyles and tibial plateau (Fig. 2). In those regions moderate density, non-uniformly distributed, predominantly clustered chondrocytes were noted, often within a fibrous surface. Pronounced degenerative changes were also observed on the centro-medial aspect of the patella, but aside from this central region, the patella scored better than the condylar and tibial cartilage in all three modalities overall.

Table II
Pearson correlations for OA grades (N = 44)

Modality	Measure	ICRS	Histo	LSCA
ICRS	Pearson correlation	1	0.511**	0.339*
	Sig. (two-tailed)		<0.001	0.024
Histo	Pearson correlation	0.511**	1	0.405**
	Sig. (two-tailed)	<0.001		0.006
LSCA	Pearson correlation	0.339*	0.405**	1
	Sig. (two-tailed)	0.024	0.006	

**Correlation is significant at the 0.01 level (two-tailed). *Correlation is significant at the 0.05 level (two-tailed).

HISTOLOGICAL AND IMMUNOHISTOCHEMICAL OUTCOMES

The entire condylar surface was characterised by cartilage exhibiting clonal cell clustering and surface irregularities, both hallmarks of osteoarthritic change (Fig. 3) However, the structure of the cartilage varied greatly between differential load-bearing sites. In particular, the centro-lateral regions of the central and posterior load-bearing aspects of the medial femoral condyle appeared to possess many more surface disruptions and fissures than the adjacent cartilage areas (Fig. 4). As in the femoral condyle, the entire patellar surface was characterised by cartilage exhibiting clonal cell clustering, but with obvious structural variation. Most sites depicted complete cartilage disorganisation or fissures extending into the radial and calcified zones of the cartilage. Interestingly, the central patellar regions exhibited only minor surface irregularities compared to the complete disorganisation and fissures observed in the medial and lateral regions (Fig. 2). Clonal cell clustering was widespread across the tibial surface with highly variable cartilage structure, although some structural uniformity was seen in the lateral region of the medial tibia. The centro-lateral regions of the central and posterior load-bearing aspects of the tibial plateau were characterised by cartilage with fissures extending into the transitional zone. These regions correlated to the opposing surface regions on the medial femoral condyle that scored similarly, suggesting cartilage sequelae from medial compartment joint space narrowing; a typical clinical presentation in OA knees.

ASSESSMENT CORRELATION

Qualitative correlation was made by comparing similar tissue features between LSCA images and H&E histology (Figs. 3 and 4). Classical histological features such as chondrocyte clustering (CC), surface fibrillation, and fissure formation were all readily apparent in corresponding sites between both microscopic imaging modalities. However as might be expected, arthroscopic ICRS assessment often underestimated the degree of OA degenerative changes in comparison to both LSCA and histological assessment.

STATISTICAL ANALYSIS

ICC analysis demonstrated ''fair agreement'' between ICRS and modified-Mankin assessment (ICC = 0.568, 0.212–0.764), ''moderate agreement'' between ICRS and LSCA (ICC = 0.354, 0.178–0.647), and ''fair agreement'' between modified-Mankin and LSCA (ICC = 0.5712, 0.218–0.765). Pearson correlation analysis demonstrated a moderate yet statistically significant ($P < 0.05$) positive correlation between all modalities (Table II), suggesting a possible role for LSCA in assessing OA change.

Discussion

In the continuing effort to improve our understanding of the aetiology, diagnosis, and prognosis of OA, some authors have indicated the need for a more accurate, non-destructive cartilage imaging and diagnosis method[29]. Further, it has been suggested that current diagnostic methods may lack the sensitivity required to detect the earliest changes in OA[30]. The LSCA has been previously shown

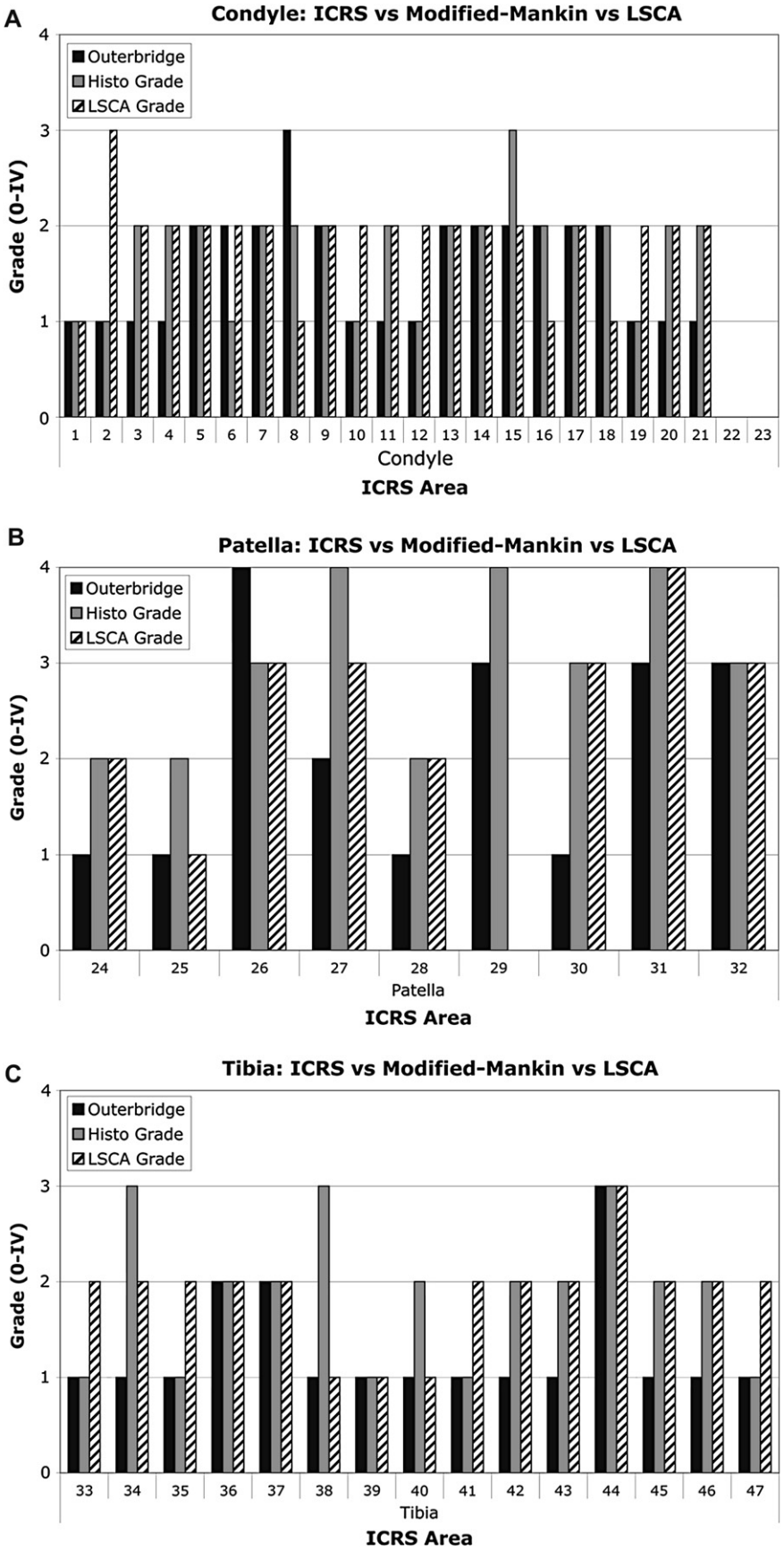

Fig. 2. OA grades (I–IV) from ICRS, LSCA and modified-Mankin histological assessment for the femoral condyles, tibial plateau and patella. OA grading of (A) femoral condyle sectors, (B) patella sectors and (C) tibial sectors. Both condylar and tibial cartilage were generally Grade II OA, while patella cartilage was mainly Grade III OA.

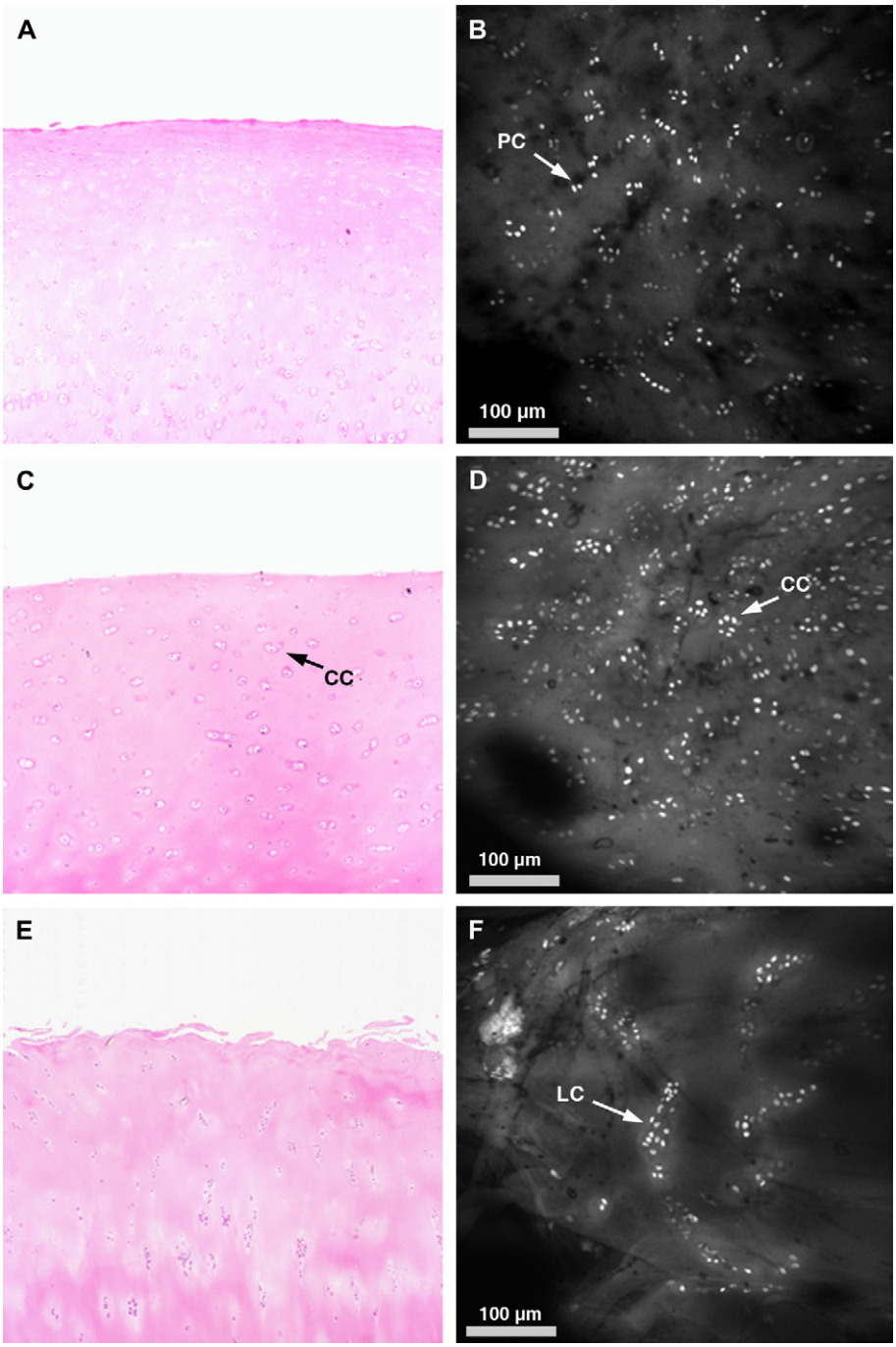

Fig. 3. Healthy and OA (Grades I–II) histology compared to LSCA imaging of corresponding region. (A) H&E histology (40×) and (B) LSCA imaging of native healthy AC, demonstrating paired chondrocytes (PC) uniformly distributed in the superficial zone. (C) H&E histology (40×) and (D) LSCA imaging of Grade I OA with CC and increased cellular density. (E) H&E histology (40×) and (F) LSCA imaging of Grade II OA demonstrating surface fibrillation, loss of uniform cellular distribution, low cell density and large clumped clusters (LC) of chondrocytes. LSCA imaging illustrated the predominance of large chondrocyte clusters in the superficial zone. *Note*: LSCA images are *XY* slices (i.e., coronal) vs *XZ* histology (i.e., cross-sectional), dark shadows in lower left quadrant are image artefacts as a result of lens marking.

to enable the non-destructive *in vivo* imaging of AC, bone, ligament, muscle, menisci and synovium[18]. The LSCA has also been demonstrated to enable accurate morphological analysis of individual chondrocytes and has shown promise in the field of OA research[31,32]. The LSCA is unique in its applicability in orthopaedic research, due to its ability to generate high detail 2D and 3D images of tissue microstructure *in situ*, thereby obviating the need for destructive mechanical biopsy. In this study, we have demonstrated the feasibility of using the LSCA in a human knee joint for the non-destructive assessment of cartilage histology *via* optical biopsy. We have shown that the LSCA enables visualisation of cellular morphology and cellular distribution in OA AC. The histological features obtained from LSCA are correlated with

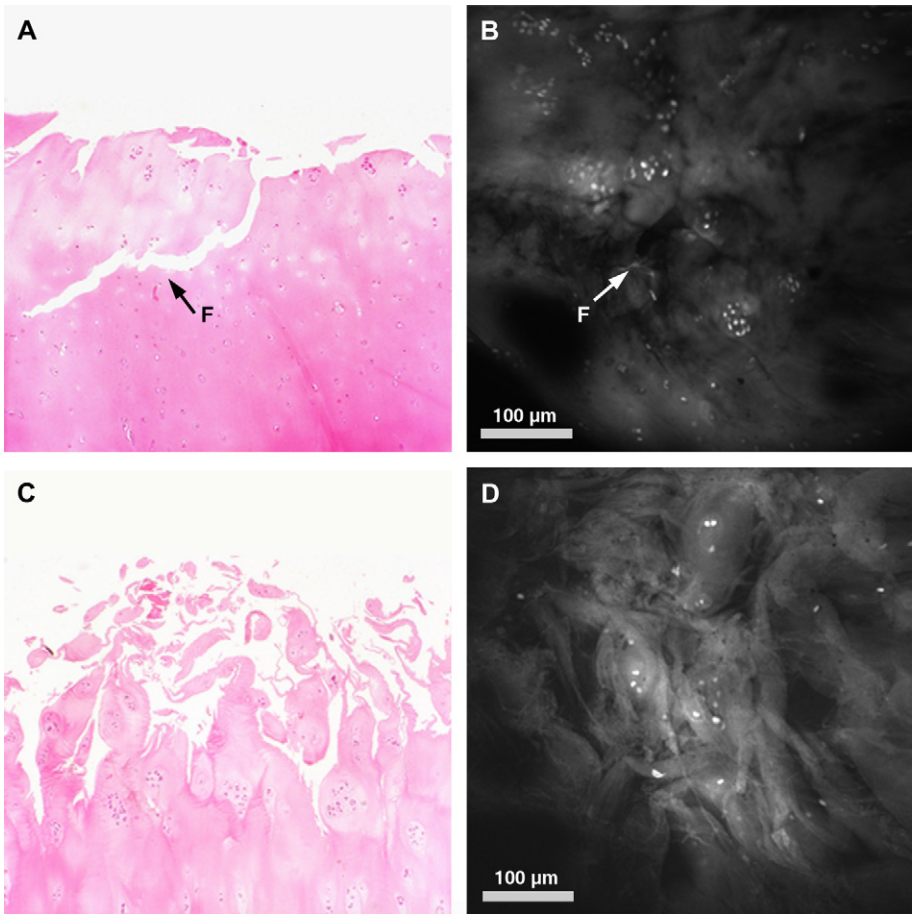

Fig. 4. Healthy and OA (Grades III–IV) histology compared to LSCA imaging of corresponding region. (A) H&E histology (40×) and (B) LSCA of Grade III OA, demonstrating severe surface fibrillation, deep cartilage fissuring (F) with clustered chondrocytes, and reduced cellularity visible. (C) H&E histology (40×) and (D) LSCA of Grade IV OA, with complete disruption of normal chondral architecture and almost total loss of chondrocytes apart from sparse clustering. LSCA imaging illustrates the gross fibrillation and mostly acellular nature of the cartilage surface.

traditional H&E paraffin embedding histology. While our data is limited by the assessment of single cadaveric knee joint, nevertheless our study has shown for the first time that the LSCA can be used for the assessment of human cartilage structure *in situ*.

The validity of histopathological grading of cartilage from OA knee joints has been previously demonstrated and the classification of OA severity by modified-Mankin scoring system has been validated with high inter- and intra-observer agreement, however the destructive nature of histological biopsy remains a limiting factor[27,33]. Poole[13] has suggested that techniques introducing trauma to the articular surface of a synovial joint should ideally not be used for long-term human investigations. Also, the process of biopsy sampling for histology can involve problems related to inadequate sample quality, with a reported 55% of specimens examined by the ICRS considered to be of unsuitable quality due to incomplete depth or fragmentation of the sample[34]. While mechanical biopsy is obviously useful in assessing cartilage treatment options in partial thickness lesions, the LSCA may be more useful in full thickness defects with a lack of tissue suitable for biopsy. Despite these drawbacks histology remains the gold standard, however recent developments in non-destructive assessment of AC may eventually obviate the need for mechanical biopsy. In particular, arthroscopic optical coherence tomography (AOCT) as described by Chu *et al.*[36] is similar to the LSCA in that it provides non-destructive assessment of AC *via* optical biopsy. Like the LSCA, the AOCT has been used to assess native AC, cartilage repair treatments and osteoarthritic cartilage in comparison to conventional histology[35,36]. The AOCT system differs considerably from the LSCA in that it utilises an echographic interpretation of near-infrared light to generate cross-sectional images of tissue, rather than the confocal microscopy employed by the LSCA. While providing good correlation to histology, the 10 μm axial resolution of the AOCT currently limits its application to the detection of surface fibrillations, which are acknowledged as relatively late changes in OA[23]. In contrast to the LSCA (which has an axial resolution of 2 μm), the AOCT is unable to provide images on a cellular level and therefore cannot be used to detect the early chondrocyte changes that are hallmarks of OA[23].

In order to generate useful and comparable data from different research centres, Ostergaard *et al.*[33] have suggested that a new standardised approach is required for sampling, topographically describing and grading AC degeneration. The qualitative and quantitative results of our study suggest that the LSCA, used in conjunction with standard video arthroscopic investigation, may offer such an alternate approach. In this study, the LSCA was able to reproducibly identify the hallmarks of progressive OA development, from

the earliest chondrocyte clustering in low grade OA, to the gross acellular and fissured cartilage degeneration of later stage OA. While the inherent depth limitation of confocal imaging (200–300 μm) restricts assessment to the superficial and transitional cartilaginous zones of intact AC, the earliest changes in OA are thought to occur in these regions[19]. Pearson correlation analysis demonstrated a significant degree of inter-modality agreeance between ICRS, LSCA and histological grading, although as expected (given their comparable scale) the relationship was the strongest between LSCA and modified-Mankin grading. As an element of further studies, a larger sample of LSCA OA images (from multiple specimens) should be randomised and blinded to enable inter- and intra-observer correlations to be calculated. We have previously utilised the LSCA to non-destructively assess MACI[20]. Inter-observer variability (ICC) analysis of randomised blinded LSCA scores for MACI demonstrated substantial to almost perfect agreement between observers using a variation of the scoring system used in the current study.

Prior to future *in vivo* imaging in human subjects, some further issues need to be addressed, including the possible toxicity of fluorophores. Fluorescein is the only suitable fluorescent contrast agent currently approved for direct systemic application in human subjects and the use of fluorescein in a multitude of procedures is widely appreciated. In contrast, acridine orange differentiates specific DNAs and RNAs in nuclei and cytoplasm and has been demonstrated to have distinct cellular effects including inhibition of mitosis and the induction of bi-nucleation in chondrocytes[37]. It has also been noted that the combination of intense laser light illumination and potential fluorophore toxicity may be damaging to living cells[38]. Hence, the safety of this technique must be confirmed before any widespread clinical use can be advocated, and this remains the focus of ongoing studies.

In this study, we have demonstrated the viability of the LSCA for non-destructive arthroscopic confocal imaging of the microstructure of OA knee cartilage and its potential to obviate the need for destructive mechanical biopsy. In this role, the LSCA is potentially an extremely valuable research and clinical tool for the assessment of AC microstructure in patients, especially in relation to elucidating the aetiology of early OA.

Acknowledgements

This work was supported by grants from the Australian Research Council SPRIT Grant (Project ID: C00107367). The researchers are grateful for the LSCA equipment supplied by Optiscan Pty Ltd., Mount Waverley MDC, Victoria 3149, Australia. Cadaveric material purchased through CTEC, University of Western Australia Campus, Crawley, Perth, WA 6009, Australia.

References

1. Hunziker EB, Quinn TM, Hauselman H-J. Quantitative structural organization of normal adult human articular cartilage. Osteoarthritis Cartilage 2002;10:564–72.
2. Wong M, Wuethrich P, Eggli P, Hunziker E. Zone-specific cell biosynthetic activity in mature bovine articular cartilage: a new method using confocal microscopic stereology and quantitative autoradiography. J Orthop Res 1996;14:424–32.
3. Gardner DL, Salter DM, Oates K. Advances in the microscopy of osteoarthritis. Microsc Res Tech 1997; 37:245–70.
4. Walker JM, Bernick S. Natural ageing and exercise effects on joints. In: Helminen HJ, Kiviranta I, Tammi M, Eds. Joint Loading. Bristol, England: Wright 1987:89–111.
5. Oddis CV. New perspectives in osteoarthritis. Am J Med 1996;100:10S–5S.
6. Poole AR, Kojima T, Yasuda T, Mwale F, Kobayashi M, Laverty S. Composition and structure of articular cartilage: a template for tissue repair. Clin Orthop Relat Res 2001;1:S26–33.
7. Frenkel SR, Di Cesare PE. Degradation and repair of articular cartilage. Front Biosci 1999;4:d671–85.
8. Vignon E, Arlot M, Patricot LM, Vignon G. The cell density of human femoral head cartilage. Clin Orthop 1976;121:303–8.
9. Meachim G, Ghadially FN, Collins DH. Regressive changes in the superficial layer of human articular cartilage. Ann Rheum Dis 1965;24:23–30.
10. Mitrovic D, Quintero M, Stankovic A, Ryckewaert A. Cell density of adult human femoral condylar articular cartilage. Lab Invest 1983;49:309–16.
11. Stockwell RA. The interrelationship of cell density and cartilage thickness in mammalian articular cartilage. J Anat 1971;109:411–21.
12. Sandy JD, Barrach HJ, Flannery CR, Plaas AH. The biosynthetic response of the mature chondrocyte in early osteoarthritis. J Rheumatol 1987; Suppl 14: Spec No: 16–19.
13. Poole AR. What type of cartilage repair are we attempting to attain? J Bone Joint Surg Br 2003;85-A:40–4.
14. Moskowitz R. Clinical and laboratory findings in osteoarthritis. In: Koopman WJ, Ed. Arthritis and Allied Conditions: A Textbook of Rheumatology. Baltimore: Williams & Wilkins 1997:1985–2011.
15. Buckland-Wright JC. Current status of imaging procedures in the diagnosis, prognosis and monitoring of osteoarthritis. Baillieres Clin Rheumatol 1997;11: 727–48.
16. Altman RD, Kates J. Arthroscopy of the knee. Semin Arthritis Rheum 1983;13:188–99.
17. Blackburn WD, Chivers S, Bernreuter W. Cartilage imaging in osteoarthritis. Semin Arthritis Rheum 1996; 25:273–81.
18. Jones CW, Keogh A, Smolinski D, Wu JP, Kirk TB, Zheng M-H. Histological assessment of the chondral and connective tissues of the knee by confocal arthroscope. J Musculoskelet Res 2004;8:75–86.
19. Jones CW, Smolinski D, Keogh A, Kirk TB, Zheng M-H. Confocal laser scanning microscopy in orthopaedic research. Prog Histochem Cytochem 2005;40:1–71.
20. Jones CW, Willers C, Keogh A, Smolinski D, Fick D, Yates P, *et al.* Matrix-induced autologous chondrocyte implantation (MACI) in sheep: assessment by confocal arthroscopy. J Orthop Res, in press.
21. Delaney PM, Harris MR, King RG. Fibre-optic laser scanning confocal microscopy suitable for fluorescence imaging. Appl Opt 1994;33:573.
22. Delaney PM, Harris MR, King RG. Novel microscopy using fibre optic confocal imaging and its suitability for subsurface blood vessel imaging *in vivo*. Clin Exp Pharmacol Physiol 1993;20:197–8.
23. Brittberg M, Winalski CS. Evaluation of cartilage injuries and repair. J Bone Joint Surg Br 2003;85-A:58–68.
24. Outerbridge RE. The etiology of chondromalacia patellae. J Bone Joint Surg Br 1961;43:752–7.
25. Guilak F. Compression-induced changes in the shape and volume of the chondrocyte nucleus. J Biomech 1995;28:1529–41.

26. Arnoczky SP, Lavagnino M, Whallon JH, Hoonjan A. *In situ* cell nucleus deformation in tendons under tensile load; a morphological analysis using confocal microscopy. J Orthop Res 2002;20:29–35.
27. van der Sluijs JA, Geesink RGT, van der Linden AJ, Bulstra SK, Kuyer R, Drukker J. The reliability of the Mankin score for osteoarthritis. J Orthop Res 1992; 10:58–61.
28. Bellamy N. Osteoarthritis clinical trials: candidate variables and clinimetric properties. J Rheumatol 1997; 24:768–78.
29. Pastoureau P, Leduc S, Chomel A, De Ceuninck F. Quantitative assessment of articular cartilage and subchondral bone histology in the meniscectomized guinea pig model of osteoarthritis. Osteoarthritis Cartilage 2003;11:412–23.
30. Kouri JB, Argüello C, Luna J, Mena R. Use of microscopical techniques in the study of human chondrocytes from osteoarthritic cartilage: an overview. Microsc Res Tech 1998;40:22–36.
31. Smolinski D, Wu JP, Jones CW, Zheng M-H, O'Hara LJ, Miller K, *et al*. The confocal arthroscope as a cartilage optical biopsy tool. Osteoarthritis Cartilage 2003;S111–2.
32. Jones CW, Smolinski D, Wu JP, Miller K, Kirk TB, Zheng MH. Quantification of chondrocyte morphology by confocal arthroscopy. J Musculoskelet Res 2004;8: 145–55.
33. Ostergaard K, Andersen CB, Petersen J, Bendtzen K, Salter DM. Validity of histopathological grading of articular cartilage from osteoarthritic knee joints. Ann Rheum 1999;58:208–13.
34. Mainil-Vartlet P, Aigner T, Brittberg M, Bullough P, Hollander AP, Hunziker EB, *et al*. Histological assessment of cartilage repair: a report by the histology endpoint committee of the International Cartilage Repair Society (ICRS). J Bone Joint Surg Am 2003;85-A: 45–57.
35. Chu CR, Lin D, Geisler JL, Chu CT, Fu FH, Pan Y. Arthroscopic microscopy of articular cartilage using optical coherence tomography. Am J Sports Med 2004;32:699–709.
36. Han CW, Chu CR, Adachi N, Usas A, Fu FH, Huard J, *et al*. Analysis of rabbit articular cartilage repair after chondrocyte implantation using optical coherence tomography. Osteoarthritis Cartilage 2003;11:111–21.
37. Kusuzaki K, Takeshita H, Murata H, Hashiguchi S, Nozaki T, Emoto K, *et al*. Acridine orange induces binucleation in chondrocytes. Osteoarthritis Cartilage 2001;147–51.
38. Buckwalter JA. Articular cartilage injuries. Clinl Orthop Relat Res 2002;21–37.